national accelerator laboratory

FN-259
2200

ENRICHED PARTICLE BEAMS FOR THE BUBBLE CHAMBERS AT THE FERMI NATIONAL ACCELERATOR LABORATORY

W. W. NEALE*

June 24, 1974

1. INTRODUCTION

The properties of the N3 beam line which transports particles to the 30 inch Bubble Chamber and of the N5 beam line which transports particles to the 15 foot Bubble Chamber at the Fermi National Accelerator Laboratory have been described by Lach and Pruss[1]. Both beam lines can transport charged particles at momenta up to 500 GeV/c and although the solid angle acceptance of 0.3μsr. and momentum bite of $\pm$ 0.5% $\delta p/p$ are low nevertheless adequate fluxes of protons and negative pions are available at most momenta[2] up to the momentum of the extracted proton beam.

Ultimately both beam lines will have a particle tagging system based on two Cerenkov Counters and a series of proportional wire chambers which should enable pions, kaons and protons to be tagged reliably at momenta up to well over 200 GeV/c.[3] However since Kaons and Antiprotons constitute at most just a few per cent of the particles arriving at the bubble chambers then even with tag-

ging it would take rather a long time to accumulate a significant number of events in the chambers.

For this reason various schemes are proposed for increasing the proportion of wanted particles in the beams arriving at the bubble chambers. Some of the ideas have been tested and shown to work and preliminary results will be presented later on in this report. The schemes to be described involve a) particle filtering b) multiple targetting and c) use of the target halo and will each be discussed in some detail.

To keep the number of protons required at the target to a minimum it is proposed that additional quadrupoles be used to increase both the solid angle acceptance and momentum bite of the beam lines. It is probably desirable to do this whether or not experiments needing enriched particle beams are requested.

The modifications to the beam lines which are described later would in theory lead to tagged enriched $\pi^{\pm}$, $K^{\pm}$, p and $\bar{p}$ beams being available over a wide range of momentum at either bubble chamber at short notice and would constitute a generally available facility.

2. THE STANDARD BEAM LINES

The beam lines contain magnets, collimators and detectors which are grouped together in Enclosures. N3 and N5 have a first stage in common and start to diverge in Enclosure 103. The distance between the target and the bubble chambers is approximately 1,000 metres.

The estimated fluxes of π^+, π^-, K^+, K^-, p and $\bar{p}$ which could

in theory be delivered to the bubble chambers are given in Fig. 1. It has been assumed that 10" protons of momentum 300 GeV/c are incident on a 12 inch long Beryllium Target and that a production angle of 0 mr. is used. The particle yields measured by Baker et al[4] have been taken as a starting point.

An acceptance $\delta\Omega . \delta p/p$ of 3×10^{-9} sr has been assumed and corrections made for decay losses and the difference in production angle. A fall off of flux with increasing transverse momentum as shown in Fig. 2 has been assumed.[5]

The proportions of π^+, K^+ and p in positive beams and of π^-, K^- and p in negative beams arriving at the bubble chambers are given in Fig. 3. These are based on the measurements of Baker et al[4] at a production angle of 3.6 mr and are expected to be slightly different at other angles.

3. INCREASED ACCEPTANCE

The solid angle acceptance of the beam lines is at present determined by the Quadrupole Doublet in Enclosure 101. It is suggested that the acceptance can be significantly improved by adding a Quadrupole Doublet in Enclosure 100. Another doublet in Enclosure 103 acting as a Field lens would enable this increased solid angle acceptance to be fully exploited and in addition would enable the momentum bite to be doubled.

Computations have been done assuming different types of Quadrupole magnet and at various momenta. However the ray traces shown in Figs. 4 and 5 for the N3 and N5 beam lines respectively at 200 GeV/c, which would yield a factor $\gtrsim 10$ increase in fluxes,

are based on the use of two high gradient (up to 500 $T.m^{-1}$) quadrupoles of the type developed by Elliott[6] and others in Enclosure 100 and two 3Q52 type quadrupole magnets in Enclosure 103.

Such increases in acceptance are desirable if not essential when certain enrichment schemes are used.

4. ENRICHMENT SCHEMES

a) Particle Filtering

Measurements of Hadron-Nucleon and Hadron-Nucleus total and absorption cross sections[7] yield values that are significantly different for pions, kaon, protons and antiprotons. The differences diminish with increasing atomic weight.

The various hadrons will pass out of the beam line solid angle and momentum bite at different rates when passed into any material. The amount of absorber that can usefully be used is limited by any or all of the following factors: a) incident particle flux, b) coulomb scattering losses and, c) muon contamination. The incident flux will normally be adequate and coulomb scattering losses (and coherent elastic losses) can be minimized by having the filter at a focus. Muons are not attenuated significantly by absorbers and will normally be the limiting factor.

The estimated percentages of p, π^+ and K^+ in the "accepted beam" emerging from a 40 metre long liquid Deuterium filter are shown in Fig. 6. It would appear that useful π^+ and K^+ beams could be made in this way over a large momentum range.

Recently at 200 GeV/c with an incident proton beam of momentum 300 GeV/c it was found that the normal beam arriving at

the 30" bubble chamber had a π^+/p ratio of 0.053. When a filter consisting of 12 feet of water and 18 inches of polyethylene was placed in Enclosure 103 the ratio went up to 0.387 which was an improvement by a factor $\sim 7 \cdot 3$. There were about half as many muons as pions at the bubble chamber. No significant improvement in the K^+/π^+ ratio was observed and further tests will be needed before this is understood.

Defining $x = p/p_o$ where p is the secondary particle momentum and p_o the incident proton momentum Baker et al[4] find that the π^+/p ratio falls rather rapidly with increasing x and is more or less independent of incident momentum as can be seen in Fig. 7. Thus a better π^+/p ratio can be obtained by going to a higher incident proton momentum. Assuming a water/polyethylene filter with the attenuation properties described above Table 1 gives the beam composition at various secondary momenta for different incident momenta.

To obtain really good K^+ beams by the filtering technique it appears necessary to use a Deuterium filter. Such a filter could have a variable length up to 40 metres and could be placed inside the large vacuum chamber immediately downstream of Enclosure 103.

b) Multiple Targetting

It has already been seen that when protons are incident on the target, the positive particle beams arriving at the bubble chamber consist mainly of protons and negative beams chiefly of pions. In Table 2 we indicate the dominant positive and negative

secondaries expected at large x values when various particles are incident on the target.

Production of p, π^+, K^- beams using double targetting and $\bar{p}$, K^+, K^- using triple targetting in the vicinity of the normal target position will now be discussed. The production hyperon and neutral particle beams using second targets near the bubble chambers will also be considered.

(i) Low Momentum Proton Beams

With 300 GeV/c protons incident on the target the proportion of π^+ in positive secondary beams starts to become significant below 150 GeV/c and in fact below about 100 GeV/c π^+ are the dominant particles. Tests in the N3 beam line have shown that, by placing a second target in the beam of neutrals produced in the first target, having first deflected the charged particles produced in the first target, as shown in Fig. 8, an enriched proton beam may be obtained.

In fact at 100 GeV/c and 60 GeV/c the beams arriving at the chamber were found to contain 95% and 85% protons respectively corresponding in both cases to an enrichment factor of about 20.

(ii) Positive Pion Beams

By retargetting negative pions it should be possible to obtain a positive beam consisting chiefly of positive pions but perhaps containing a significant proportion of kaons. A practical beam line layout that could be used to obtain an intense focussed beam of negative secondary particles in Enclosure 100 is shown in Fig. 9.

The proton beam from the accelerator is focussed onto a target placed 20 feet upstream of the standard target. The gradients of the quadrupoles in the proton beam line need to be increased by about 15% but the spot size should be slightly smaller. Ray traces through these 'N7' quadrupoles for the standard and upstream target positions are shown in Fig. 10.

Negative secondaries are focussed onto a second target placed about 60 feet downstream of the first one using the same type of pulsed high gradient quadrupole magnet[6] as was suggested earlier for increasing solid angle acceptance.

The steel collimator defines the solid angle accepted by these quadrupoles, being 1 μsr at 200 GeV/c. Only the second dipole is used but the deflections produced are sufficient to ensure that only negative secondaries hit the target and all positive particles, including non-interacting protons, which pass through the collimator aperture are intercepted by the beam dump. The momentum spectrum of its negative secondaries hitting the target is determined by chromatic aberrations rather than dispersion.

Assuming that the beam is focussed at 200 GeV/c onto a target with a 3mm x 3mm cross section the fraction of the secondaries within the solid angle acceptance colliding with the target is shown as a function of momentum in Fig. 11. It is seen that the effective momentum bite is ~20 GeV/c (i.e. $\delta p/_p = \pm 5\%$). A value for $\delta\Omega . \delta p/_p$ of 10^{-7}sr will be assumed for the purpose of estimating fluxes. If the beam line is left unchanged the flux of negative

particles as a function of momentum is as given in Fig. 12.

The inclusive production of π^+ in π^-p collisions has been studied at many momenta[8]. In Fig. 13 dN/dx is plotted as a function of x, the ratio of π^+ momentum to incident π^- momentum. N is the number of π^+ per incident π^- and is an estimate based on all the available data.

Assuming a momentum bite of $\pm$ ½% $\delta p/p$ in N3 or N5 and that ~20% of produced π^+ within the momentum bite are transported to the bubble chambers Fig. 14 shows the expected fluxes of 100, 150 and 200 GeV/c π^+ for various intermediate π^- momenta assuming 10" protons of momentum 300 GeV/c incident on the first target. It is seen that a wide range of intermediate π^- momenta would yield adequate fluxes.

Above 200 GeV/c a significant number of Σ^- are produced not all of which decay before reaching the second target. If these interact they will give rise to contaminating protons. To minimize proton contamination therefore the intermediate π^- momentum should be kept close to the π^+ momentum.

It would of course be possible to combine this double targetting technique with the filtering technique to produce π^+ beams with almost no proton contamination.

(iii) Negative Kaon Beams

The beam line layout used for positive pions which has just been described can also be used for negative kaons. Negative particles with momentum close to the incident proton momentum are selected. These are expected to be mainly Σ^- hyperons[9]. It is

likely that the inclusive production of K^- by Σ^- will be strong since $\delta S = \delta Q = 0$ and the K^-/π^- ratio is expected to be higher than the K^+/π^+ ratio found with incident protons.

The lack of experimental data on Σ^- production and interactions at high energies make it difficult to predict fluxes. The Σ^-/π^- ratio has been measured by Baker et al[9] at 24 GeV/c. Assuming a similar dependence on x at 300 GeV/c and allowing for decay losses about 10^5 Σ^- should arrive at the second target for 10^{11} protons incident on the first when the magnets are set to deliver 250 GeV/c negatives. With the improved acceptance versions of the beam lines adequate fluxes of K^- should be available up to at least 150 GeV/c.

(iv) Enrichment Using Elastic Scattering

Preliminary data[10] on the elastic scattering of hadrons at high energies indicates that differences may be large enough between the various particles at particular 't' values to be exploited as a means of beam enrichment. The double targetting scheme would need to be modified to enable large production angles at the second target to be selected.

(v) $\bar{p}$, K^+ and K^- Using Triple Targetting

The primary proton beam is used to produce a negative secondary beam which is retargetted in the manner previously described. Neutral particles produced by the negative secondaries are retargetted and used to produce a positive beam rich in K^+ or a negative beam rich in K^- and $\bar{p}$. Since the neutral particles

cannot be focussed they must be targetted within a short distance of the point of production. It is suggested that a pulsed dipole of the type developed by Elliott et al[6] be used to deflect charged secondaries. The coil structure of such a magnet is shown in Fig. 15 and in fact the material of the coil acts as two targets. Since the field region is only 8 inches long the displacement of charged relative to neutral secondaries is negligible. However charged secondaries are given a transverse momentum of 900 MeV/c by the magnetic field and by operating at non-zerio production angles the background due to charged particles traversing the neutral link can be minimized.

With 10^{12} incident protons it is estimated that reasonably pure K^+ or $K^-/\bar{p}$ beams could be made at around 100 GeV/c with an intensity in the range 1-10 particles/pulse. These fluxes are low compared with those expected using other schemes. Extensive testing and development will probably be necessary to optimize fluxes and minimize background.

(vi) Neutral Particle Beams

Neutral beams consisting chiefly of neutrons can be made by targetting protons near the bubble chamber. A possible layout for the 15 foot H.B.C. is shown in Fig. 16. The Quadrupoles shown are in Enclosure 115 in the N5 beam line and are horizontally focussing giving a beam at the target which is almost parallel in the vertical plane and strongly convergent in the horizontal plane.

The collimators accept a wide angle horizontally and a small

one vertically. The convergent proton beam enables the neutron beam to have fairly constant properties across the bubble chamber. The dipoles deflect the charged particles vertically into the collimators. Usually 10^2 to 10^3 incident protons would be adequate so no background problems are foreseen.

Charged Kaon and Pion primaries can be used to produce long-lived neutral kaons (K^o_L) while antiproton primaries can be used for anti-neutron beams.

All of the neutral beams will in fact contain neutrons, kaons and antineutrons in different proportions so that since mass tagging is not available for such beams and since the momentum spread is large the usefulness of such beams is doubtful.

If a target close to the bubble chamber is used the beams will also contain K^o_s, Λ^o, $\bar{\Lambda}^o$, Ξ^o and $\bar{\Xi}^o$. The attenuation of hyperon decays across the bubble chamber could be used to accurately determine total cross sections. It might also be possible to obtain useful data on elastic scattering.

(vii) Charged Hyperon Beams

The very high momentum negatives produced when protons are incident on a target are chiefly Σ^- hyperons[9]. A beam rich in Σ^- could be produced if the high momentum negatives could somehow beselected in a short distance. A possible layout which could be used to produce a 240 GeV/c Σ^- beam is shown in Fig. 17.

The N5 beam line is used to transport approximately 10^5 protons at a momentum of 300 GeV/c and focus them onto the pulsed dipole magnet. The solid angle acceptance is defined by the Tungsten Collimator which follows pulsed dipole. Most secondaries

are degraded before they produce muons capable of penetrating the shielding and arriving at the bubble chamber. The pulsed quadrupoles focus the beam in the vertical plane and since dispersion is introduced by the standard dipole a momentum analyzed beam is obtained. The spread in momentum will be $\sim^{+}_{-}$ 10 GeV/c but the measurements that can be made in the bubble chamber should enable the momentum of a particular particle to be obtained to within $\pm$ 2-5 GeV/c.

The fraction of pions and Σ^- (and Ξ^-) can be estimated from observations of hyperon decays. Individual primaries which interact cannot be identified but it should be possible to separate the inclusive behavior of Σ^- and π^- statistically. For example the proportion of Σ^- and π^- interactions will change substantially between beam entry and exit due to Σ^- decay losses so that by combining data from different parts of the chamber the properties of Σ^- andπ^- interactions may be determined.

c) Beams from the Target Halo

The secondaries from Hyperon, Antihyperon and Neutral Kaon Decay give rise to a substantial "Target Halo." Of particular interest are the $\bar{p}$ from $\bar{\Lambda}^o$ decay and π^+ from K^o_s decay, present in the halo.

(i) Antiproton Beams

For incident protons above 100 GeV/c the cross section for $\bar{\Lambda}^o$ production has been found to be about one half of the cross section for $\bar{p}$ production[11]. Assuming that the differential spectra have the same shape expected $\bar{\Lambda}^o$ yields can be obtained

from measured $\bar{p}$ yields such as those measured by Baker et al.[4]

As an example consider the production of a 100 GeV/c antiproton beam. $\bar{\Lambda}^o$'s of momenta between 107 and 132 GeV/c can yield 100 GeV/c antiprotons. Since the branching ratio for $\bar{\Lambda}^o \rightarrow \bar{p} + \pi^+$ is ~64% it can be estimated that the flux of 100 GeV/c from $\bar{p}$ decay is ~15% of those produced directly in the collisions of 300GeV/c protons with the target.

Assuming the yield of K^os is the mean of K^+ and K^- yields then a detailed calculation indicates that there will be about 12 π^- from K^os decay for every $\bar{p}$ from $\bar{\Lambda}^o$ decay.

The decay products can be referred back to the target where they appear to form a diffuse virtual source. The π^- are spread over a much larger area and have a different intensity distribution. By using the beam line collimators and vernier dipole magnets the specific parts of the halo which are richest in $\bar{p}$ may be selected. In N5 beams with up to 50% $\bar{p}$ should be obtainable whereas in N3 where target redefinition takes place only in the vertical plane the proportion will be nearer 25%.

The beam line layout is shown in Fig. 18. The first dipole enables the angle at which the incident protons hit the target to be varied. The second dipole deflects most charged particles into the beam dump. Those that pass through the hole in the dump do so at such an angle that they will strike some object further down the beam line.

Only decay products originating beyond the second dipole will be useable. It is estimated that the intensity of accepted halo $\bar{p}$ will be $\gtrsim$ 1% of directly produced $\bar{p}$ at 100 GeV/c. About 10 $\bar{p}$

are expected for 10^{11} incident protons down the standard beam lines at this momentum. It is clear that the beam line acceptance must be improved in order to go to higher momenta.

(ii) Positive Pion Beams

The layout used is the same as that described for $\bar{p}$. The potential background is protons from Λ^o decay. The virtual source at the target is observed further off axis than for $\bar{p}$ to obtain a beam rich in π^+.

5. AN ENRICHED PARTICLE BEAM FACILITY

A layout of beam elements in Enclosure 100 is shown in Fig. 19, which would permit the following possibilities.

a) N3 or N5 to be used in the standard way

b) A big increase in solid angle acceptance to be obtained.

c) All of the various multiple targetting schemes discussed in the previous section to be used or tested.

d) Beams to be obtained from the target Halo.

Four target stations are shown (T1, T2, T3 and T4). T1 is used in the multiple targetting schemes as a source of charged secondaries which are focussed by the pulsed quadrupole magnets Q1 and Q2 onto the target T4. The pulsed dipole replaces T4 in the triple targetting schemes. T2 is the standard N3/N5 target, and is used with T3 in the double targetting scheme for protons. T3 is the target to be used for the Halo Beams.

The pulsed quadrupoles Q1 and Q2 are removed when not in use, using the target traversing mechanisms. The other pair of pulsed

quadrupoles which have two possible locations Q3A, Q4A, or Q3B, Q4B are used to increase the beam line acceptance.

Two beam dumps are shown which together with other shielding should enable $\gtrsim 10^{12}$ protons per machine cycle to be used.

In Enclosure 101 it would be extremely useful to have angle defining collimators with separately controllable jaws which would enable off angle pencils of particles to be produced and tracked through the system. Using such pencil beams accurate focussing is possible[12] and misalignments and obstructions can be diagnosed. Used in conjunction with a small cross section target the phase space acceptance of the beam line can be mapped out. Collimators with Steel Jaws 3 feet long would be adequate.

In Enclosure 103 there should be the option of having a water particle filter 12 feet long inside one of the beam switch dipoles, although a liquid deuterium filter up to 40 metres long would be more efficient. To exploit fully the increase in acceptance obtainable using the pulsed quadrupole magnets in Enclosure 100 a Quadrupole "Field Lens" Doublet is also required in Enclosure 103. Quadrupoles of type 3Q52, 3Q84 or 3Q120 could be used.

The equipment needed for the neutral or hyperon beams could probably be run in on rails along the beam axes to the desired position. Adequate space exists for such a railway system upstream of the bubble chambers.

With the changes outlined above it should be possible by the end of 1974 to deliver many types of enriched particle beam to either the 30 inch or 15 foot bubble chambers. The few tests carried out so far have been encouraging.

In Table 3 the likely best methods of producing π^+, π^-, K^+, K^-, p and $\bar{p}$ at 100, 150 and 200 GeV/c are listed. As higher incident proton momenta become available and improvements to the mass tagging system are made it should be possible to extend the usefulness of the facility to much higher momenta.

REFERENCES

*On leave from Cavendish Laboratory, Cambridge, U.K.

(1) J. Lach and S. Pruss, Fermi National Accelerator Laboratory Report TM-285 (1971) "Hadron Beams in the Neutrino Area."

(2) M. Johnson, S. Kahn, D. Ljung and S. Pruss, Fermi National Accelerator Laboratory Report TM-460 (1973) "Feasibility Study for Nearly Accelerator Energy π^-p Experiments in the 30" Bubble Chamber"

(3) S. Pruss - Private Communication.

(4) W. F. Baker, D.P. Eartly, G. Giacomelli, P.F.M. Koehler, K. P. Pretzl, S.M. Pruss, A.A. Wehmann, A.S. Carroll, I-H. Chiang, T.F. Kycia, K.K. Li, P.O. Mazur, P.M. Mockett, D.C. Rahm, R. Rubinstein and O. Fackler, Fermi National Accelerator Laboratory Report NAL-Pub-74/13-EXP (1974) "Measurement of $\pi\pm$,K±, p and $\bar{p}$ production by 200 and 300 GeV/c Protons."

(5) J. Wentmore, Fermi National Accelerator Report NAL-Pub-73/70-EXP (1973). "Experimental Results on Strong Interations in the NAL Hydrogen Bubble Chamber."
P_T^2 distributions are given for $pp\rightarrow p$ and $pp\rightarrow\pi^-$ in this report. A variation somewhere between the two has been taken for the purpose of calculation.

(6) R.T. Elliott and P.S. Flower, Rutherford Laboratory Report, Nimrod (PD) 72-4 (1972) "Pulsed Magnets for A Σ^- Experiment in the CERN 2m Hydrogen Bubble Chamber."

(7) S.P. Denisov, S.V. Donskov, Yu. P. Gorin, R.N. Krasnokutsky, A.I. Petrukhin, Yu. D. Prokoshkin and D.A. Stoyanova, Nuclear Physics B61 (1973) 62. The various CERN/HERA compilations give extensive lists of references for cross section measurements in Hydrogen and Deuterium.

(8) Proceedings of the 16th International Conference on High Energy Physics (1972). On p307 of Volume 1 the x distributions for various momenta for the process $\pi^+p\rightarrow\pi^-$ ..... are plotted.

Other data is collected together in LBL-80 (1972) "A Compilation of Data on Inclusive Reactions."

(9) J. Badier, R. Bland, J.C. Chollet, T. Devlin, J-M. Gaillard, J. LeFrancois, B. Merkel, R. Meunier, J.-P. Repellin, G. Sauvage and R. Vanderhaghen, Physics Letters 39B(1972)414.

(10) C.W. Akerlof, R. Kotthaus, J.A. Koschek, R.L. Loveless, D.I. Meyer, I. Ambats, W.T. Meyer, C.E.W. Ward, D.P.Eartly, R.A. Lundy, S.M. Pruss, D.D. Yovanovitch and D.R. Rust, Paper submitted to the London Conference (1974) on High Energy Physics. "Elastic Scattering at 100 and 200 GeV/c"

(11) J. Whitmore, ibid. Results on $\bar{\Lambda}^{o}$ production and on $\bar{\Lambda}^{o}/\bar{p}$ ratio are given in this report.

(12) W. Blum, M. Jobes, D.B. Miller, W.W. Neale and J.G. Rushbrooke, Nuclear Inst. and Methods 77 (1970) 203.

TABLE 1

"BEAM COMPOSITIONS AT THE BUBBLE CHAMBER USING THE WATER PARTICLE FILTER"

Secondary Momentum (GeV/c)	Primary Momentum (GeV/c)	Composition %		
		π^+	K^+	P
100	200	53.8	2.9	43.3
	300	81.4	3.1	15.5
	400	88.6	3.0	8.4
150	300	54.5	4.4	41.2
	400	75.8	4.6	19.6
200	300	24.0	4.2	71.8
	400	54.6	5.3	40.1
250	400	31.0	5.3	63.7

TABLE 2

"DOMINANT PARTICLES PRODUCED AT LARGE X VALUES FOR VARIOUS INCIDENT PARTICLES"

Particle Incident on Target	Dominant Positive Secondary	Dominant Negative Secondary
P	P	π^-
n	P	π^-
$\bar{p}$	π^+	$\bar{p}$
$\bar{n}$	π^+	$\bar{p}$
K^+	K^+	π^-
K^-	π^+	K^-
K^o_L	K^+	K^-
π^+	π^+	π^-
π^-	π^+	π^-
Σ^-	P	K^-

TABLE 3

"SUMMARY OF BEST METHODS OF PRODUCING SECONDARY PARTICLES OF VARIOUS TYPES IN ORDER OF USEFULNESS"

(300 GeV/c Incident Protons Unless Stated Otherwise)

Particles	P = 100 GeV/c	P = 150 GeV/c	P = 200 GeV/c
P	1. Double targetting using neutrals 2. Halo from Λ^o decay 3. Direct	As for 100 GeV/c	As for 100 GeV/c
π^-	1. Direct 2. Halo from K^os Decay	As for 100 GeV/c	As for 100 GeV/c
π^+	1. Double targetting using negatives 2. Filter 3. Halo from K^os Decay	1. Double targetting using negatives 2. Filter	1. Double targetting using negatives 2. Filter Direct Beam
K^-	Double targetting using Σ^- primaries	As for 100 GeV/c	As for 100 GeV/c
K^+	1. Double targetting with π^- (+ Filter) 2. Filter Direct Beam	As for 100 GeV/c	As for 100 GeV/c
p	Halo from $\bar{\Lambda}^\circ$ Decay	As for 100 GeV/c	Use 400 GeV/c primaries and $\bar{\Lambda}^\circ$ Halo

FIGURE CAPTIONS

Fig. 1 Fluxes of p, π^+, π^-, K^+, K^- and $\bar{p}$ arriving at the Bubble Chambers when the full acceptance of the standard N3/N5 beam lines is used.

Fig. 2 Plot showing the particle flux expected at a particular transverse momentum relative to the flux at $P_T = 0$.

Fig. 3 Curves show the proportions of p, π^+ and K^+ in positive beams and of $\bar{p}$, π^- and K^- in negative beams expected at the bubble chambers at different momenta.

Fig. 4 Ray traces through the improved N3 beam line. The rays labelled 1.2 α_{12} and 0.83 α_{34} correspond to particles leaving the centre of the target at angles θ_H = 1.2 mr and θ_V = 0.83 mr. The ray α_{16} shows the displacement of the beam axis for particles with $\delta p/p$ = 1%. The other rays $0.04\alpha_{11} + \alpha_{12}$ and $0.04\ \alpha_{33}$ correspond to particles leaving the extreme edges of the target which pass through the centre of the angle defining collimators.

Fig. 5 Same as Fig. 4 but for the improved N5 beam line.

Fig. 6 Proportions of π^+, K^+ and p in beams arriving at the bubble chamber after passage through a 40 m. long liquid Deuterium filter. The muon component is not included in the estimates.

Fig. 7 $P/_{\pi}+$ and $K^+/\pi+$ ratios at production as measured by Baker et al.[4] using 200 GeV/c and 300 GeV/c incident protons, a 12 inch long Beryllium target and a production angle 3.6 mr. The ratios are plotted as a function of x which is the ratio of the particle momentum to the incident proton momentum.

Fig. 8 (a) Schematic Layout of Beam Line Elements in Enclosure 100 used in the Double Targetting Scheme for low momentum protons. (b) Using a vertical scale expanded 200 times this diagram shows which particles from the first target will arrive at the second target.

Fig. 9 (a) Schematic Layout of Beam Line Elements in Enclosure 100 used in the Double Targetting Scheme for π^+ and K^- beams.

(b) and (c) Using an expanded vertical scale these diagrams show some of the trajectories of particles between the two targets. Note that the first standard dipole is not in use.

Fig. 10 Layout of Quadrupole Magnets and Ray Traces through the N7 beam line on to the N3/N5 target in Enclosure 100. The dashed line shows the change that occurs when targetting 20 ft. upstream of the standard target position.

Fig. 11 Shows the fraction of secondaries hitting the second target in the double targetting scheme of Fig. 10 when the pulsed quadrupole magnets are tuned to give a focus at 200 GeV/c.

Fig. 12 Plot showing the number of π^- centred on a particular momentum that hit a 3 x 3 mm^2 cross section target in the double targetting scheme of Fig. 9.

Fig. 13 A plot of $dN/_{dx}$ versus x for the inclusive processes $\pi^-p \to \pi^+ \ldots$. and $\pi^+p \to \pi^- \ldots\ldots$ based on a large amount of data.(8)

Fig. 14 Expected π^+ fluxes at the bubble chamber with different incident π^- momenta in the double targetting scheme of Fig. 9.

Fig. 15 Scale drawing of the Copper Coil of the Pulsed Dipole Magnet of Elliott et al.(6)

Fig. 16 (a) Schematic Layout of Elements in and near Enclosure 115 in the N5 beam line which could be used to produce neutral beams for the 15 foot Bubble Chamber.

(b) and (c) Using an expanded vertical scale the optical properties etc. are illustrated in the Horizontal and Vertical planes.

Fig. 17 (a) Schematic Layout of Elements in the N5 beam line just upstream of the bubble chambers in a possible 240 GeV/c Σ^- beam line.

(b) and (c) Using an expanded vertical scale the optical properties etc. are illustrated in the Vertical and Horizontal planes.

Fig. 18 (a) Schematic layout of Elements in Enclosure 100 used to produce 100 GeV/c $\bar{p}$ from $\bar{\Lambda}^o$ decays.

(b) Using an expanded vertical scale some particle trajectories are indicated.

Fig. 19 Schematic Layout of Elements in Enclosure 100 needed to provide a general hadron facility.

FIGURE 1

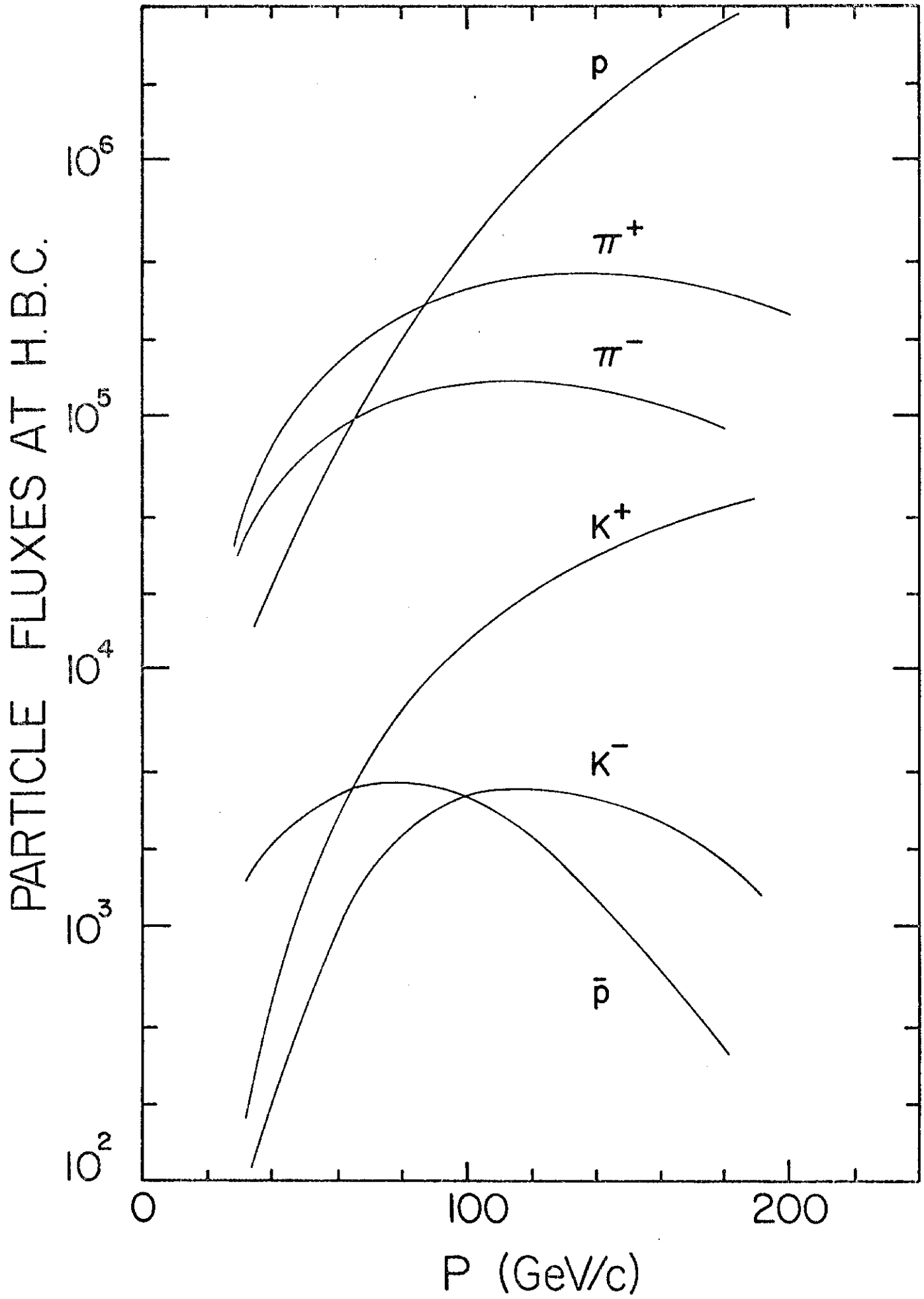
PARTICLE FLUXES AT H.B.C.
10^6
10^5
10^4
10^3
10^2
p
π^+
π^-
K^+
K^-
$\bar{p}$
0
100
200
P (GeV/c)

FIGURE 2

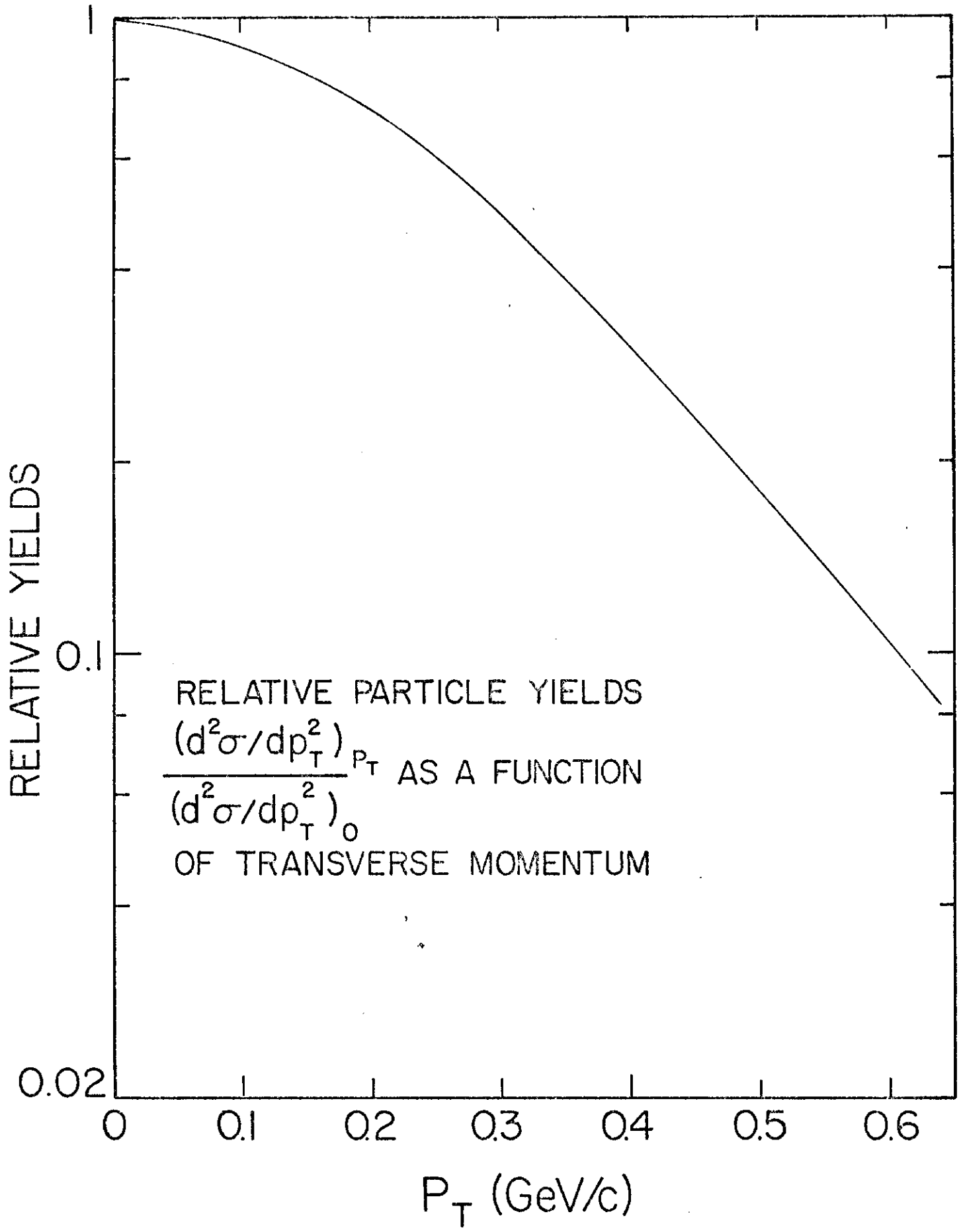
1
0.1
0.02
RELATIVE YIELDS
RELATIVE PARTICLE YIELDS
$\frac{(d^2\sigma/dp_T^2)_{P_T}}{(d^2\sigma/dp_T^2)_0}$ AS A FUNCTION
OF TRANSVERSE MOMENTUM
0
0.1
0.2
0.3
0.4
0.5
0.6
P_T (GeV/c)

FIGURE 3

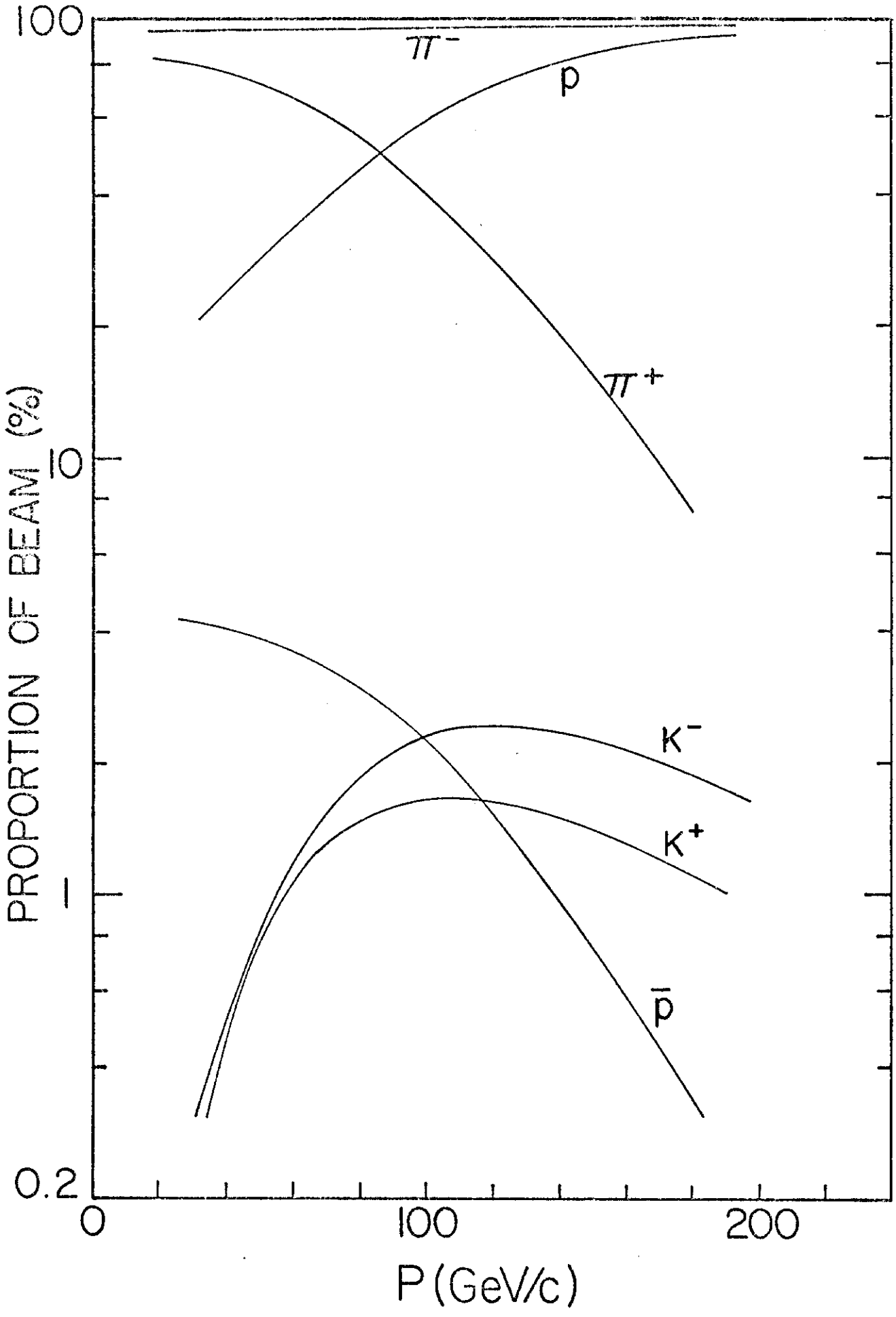

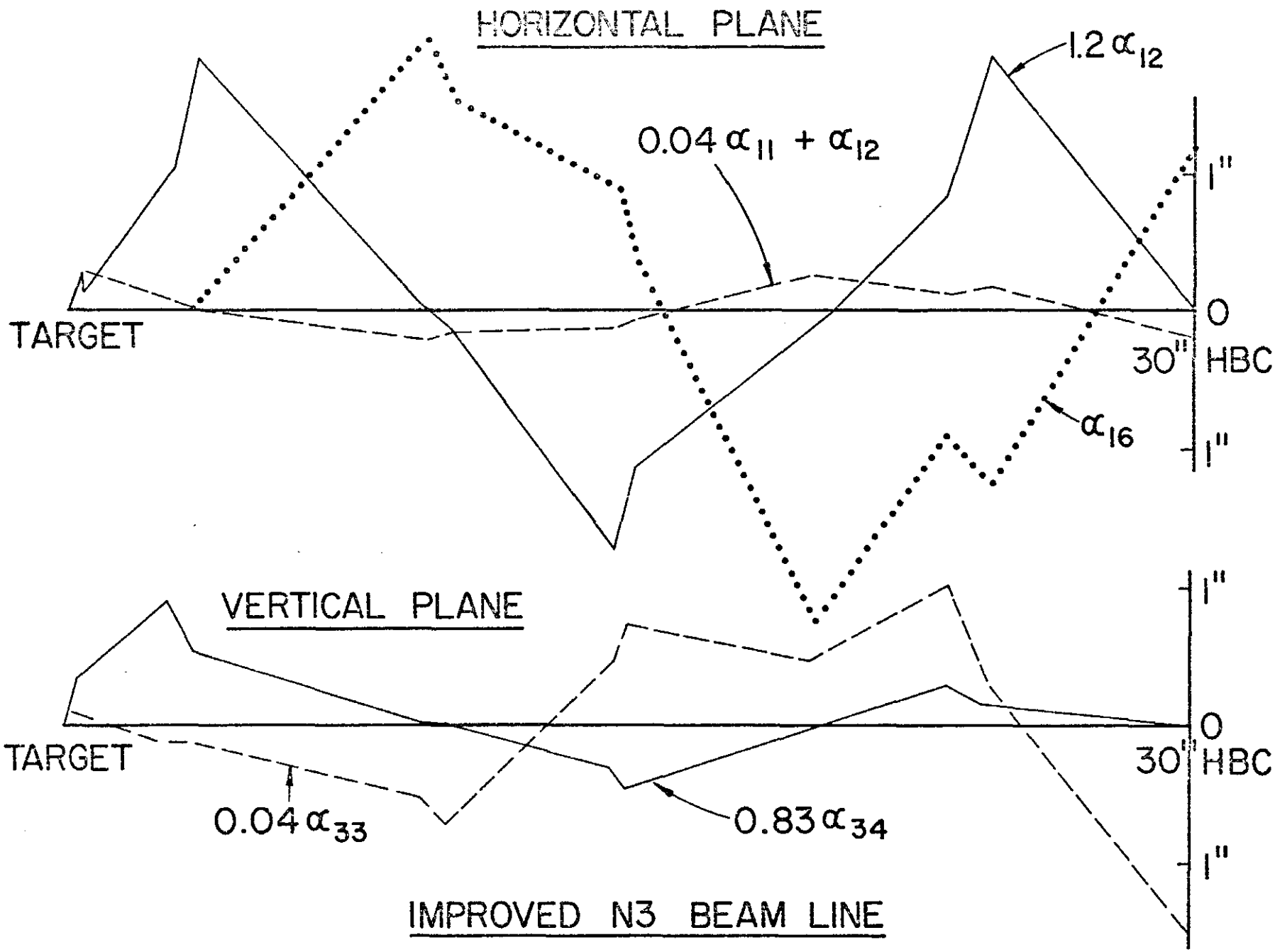
HORIZONTAL PLANE
1.2 α12
0.04 α11 + α12
1"
0
TARGET
30"
HBC
α16
1"
VERTICAL PLANE
1"
0
TARGET
30"
HBC
0.04 α33
0.83 α34
1"
IMPROVED N3 BEAM LINE

FIGURE 4

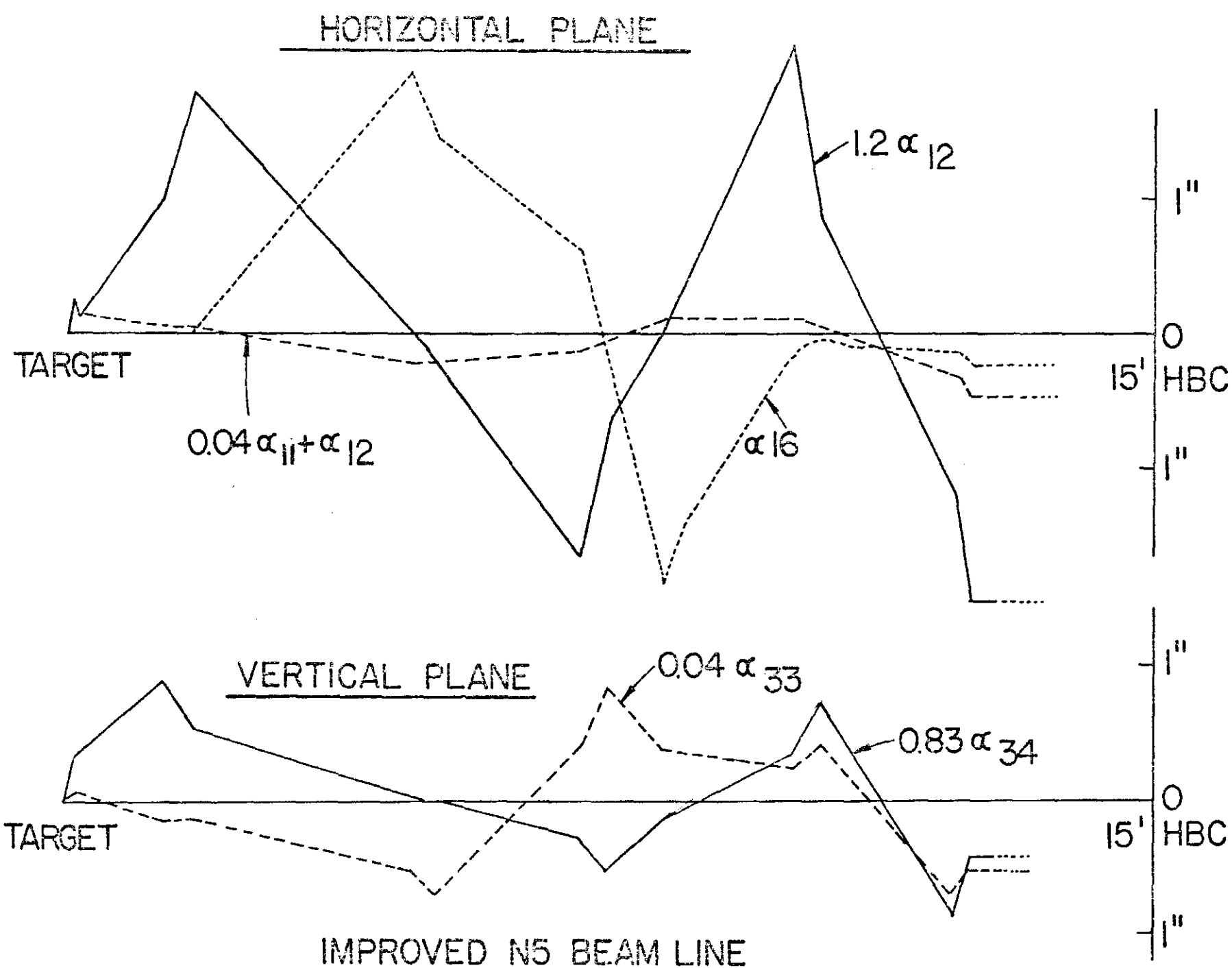
HORIZONTAL PLANE
1.2 α 12
1"
0
TARGET
15' HBC
0.04 α 11 + α 12
α 16
1"
VERTICAL PLANE
0.04 α 33
1"
0.83 α 34
0
TARGET
15' HBC
1"
IMPROVED N5 BEAM LINE

FIGURE 5

FIGURE 6

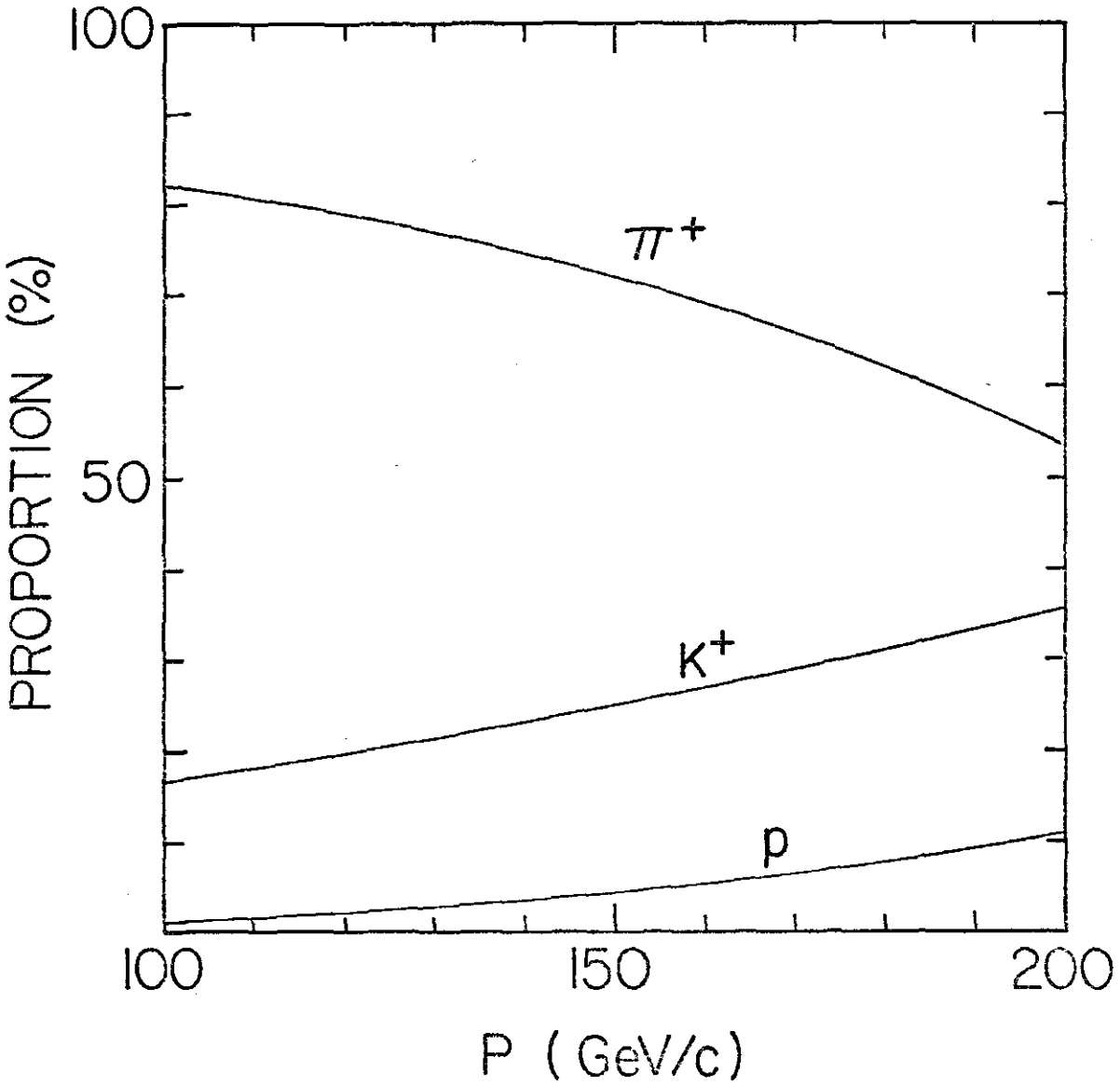

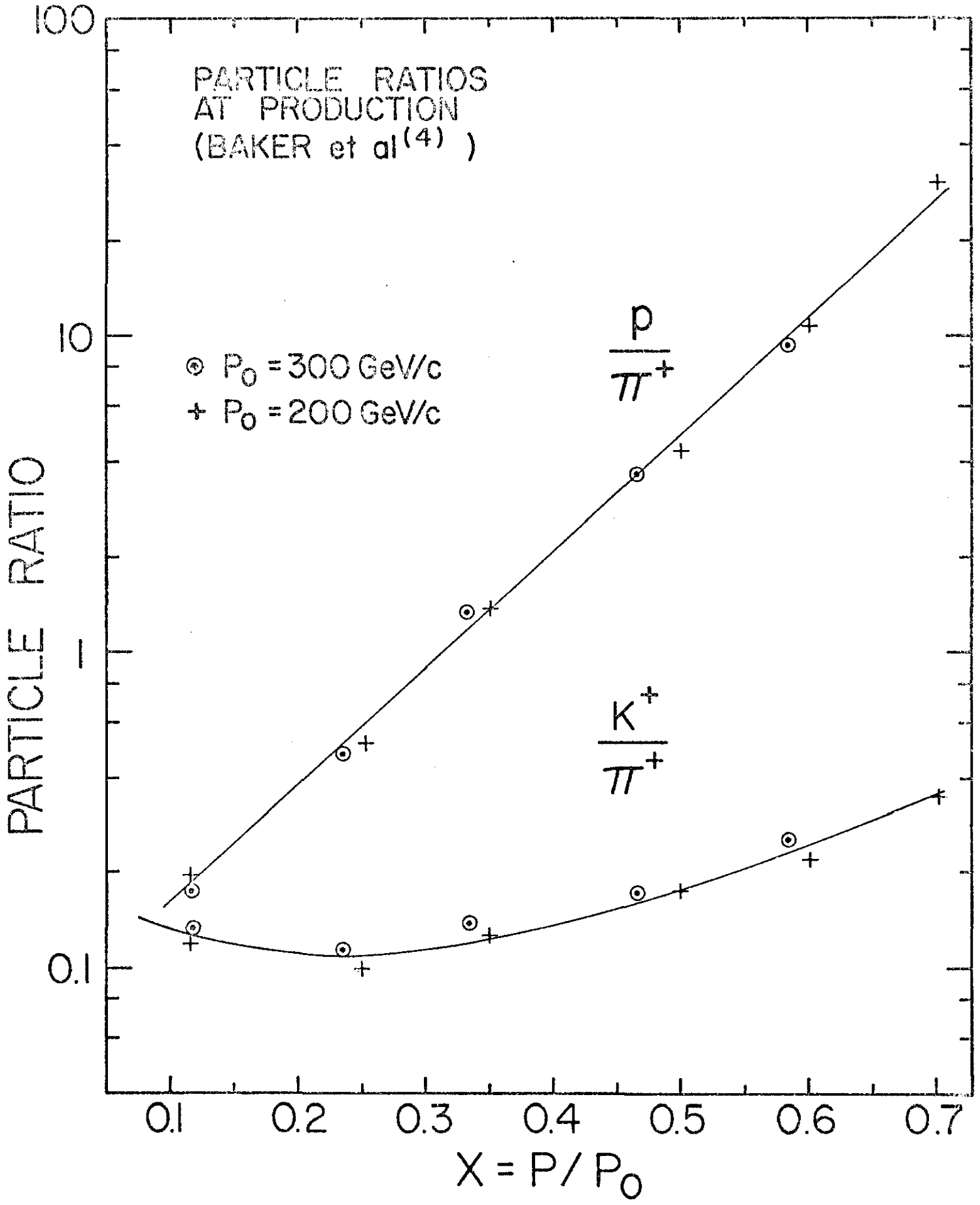
PARTICLE RATIOS
AT PRODUCTION
(BAKER et al[4])
⊙ P_0 = 300 GeV/c
+ P_0 = 200 GeV/c
$\frac{p}{\pi^+}$
$\frac{K^+}{\pi^+}$
PARTICLE RATIO
100
10
1
0.1
0.1
0.2
0.3
0.4
0.5
0.6
0.7
$X = P/P_0$

FIGURE 7

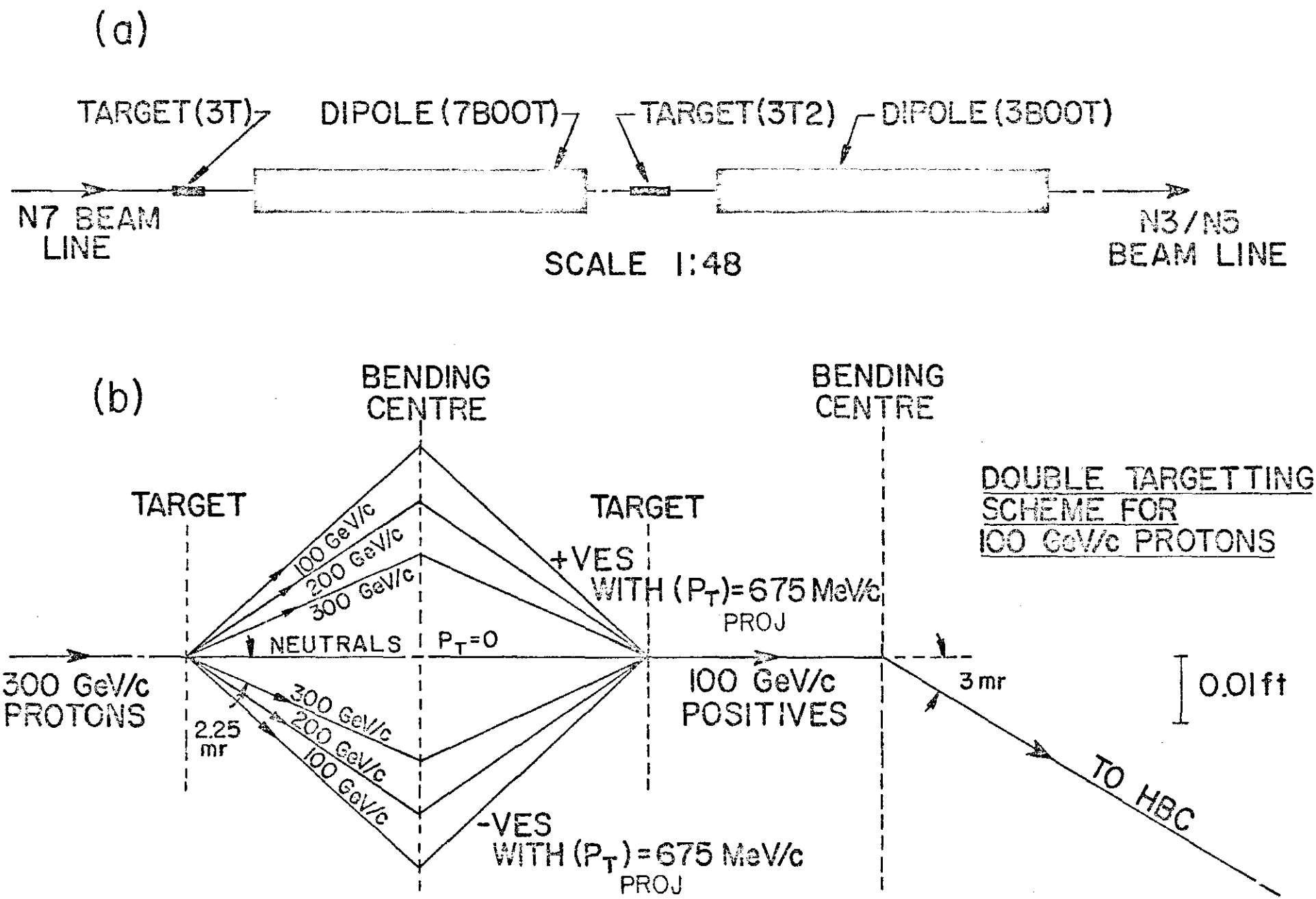
(a)
TARGET(3T)
DIPOLE(7BOOT)
TARGET(3T2)
DIPOLE(3BOOT)
N7 BEAM LINE
N3/N5 BEAM LINE
SCALE 1:48
(b)
BENDING CENTRE
BENDING CENTRE
TARGET
TARGET
DOUBLE TARGETTING SCHEME FOR 100 GeV/c PROTONS
100 GeV/c
200 GeV/c
300 GeV/c
+VES WITH (P_T)=675 MeV/c PROJ
NEUTRALS
P_T=0
300 GeV/c PROTONS
2.25 mr
300 GeV/c
200 GeV/c
100 GeV/c
100 GeV/c POSITIVES
3 mr
0.01 ft
TO HBC
-VES WITH (P_T)=675 MeV/c PROJ

FIGURE 8

FIGURE 9

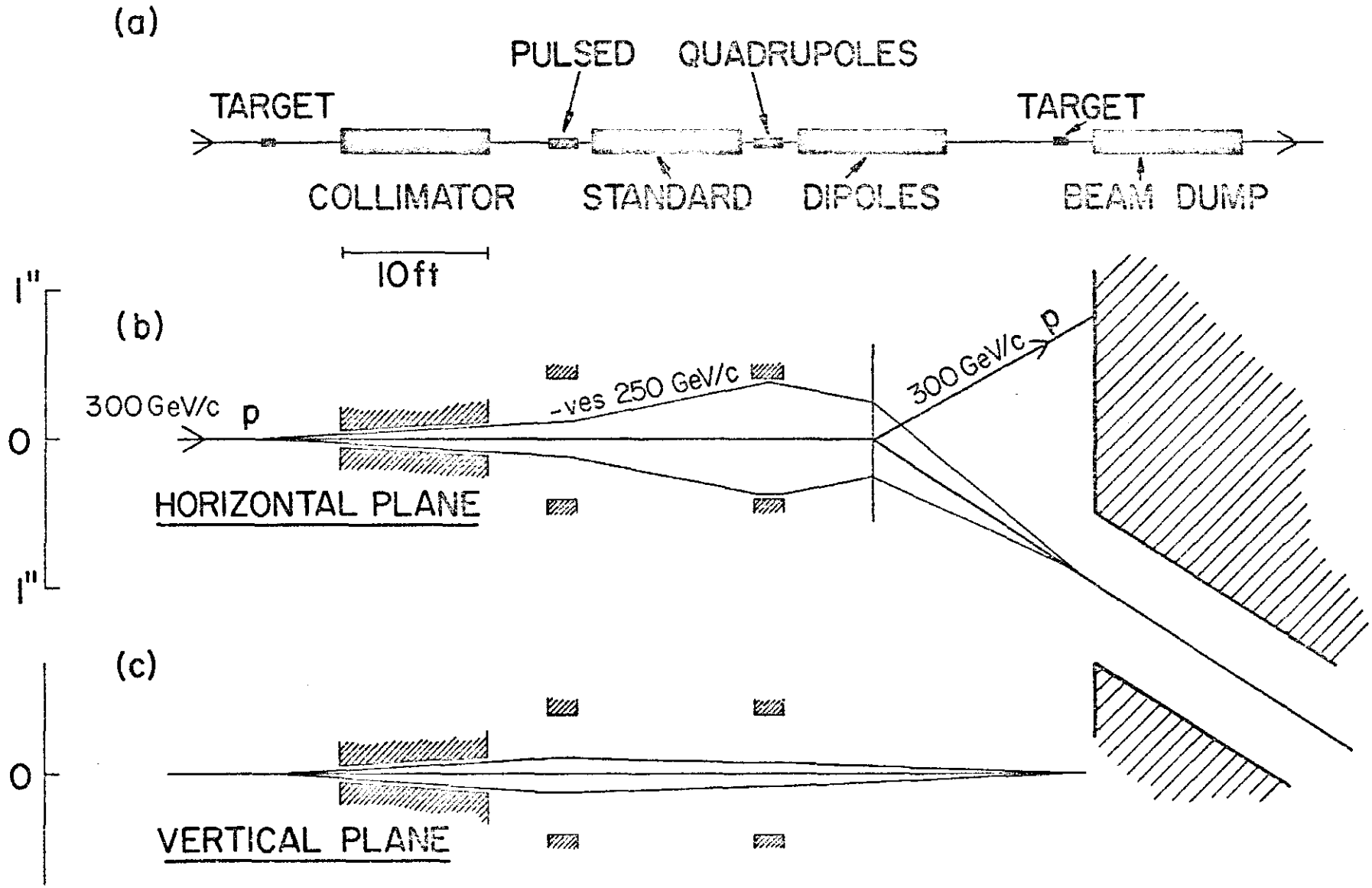

DOUBLE TARGETTING LAYOUT AND OPTICS

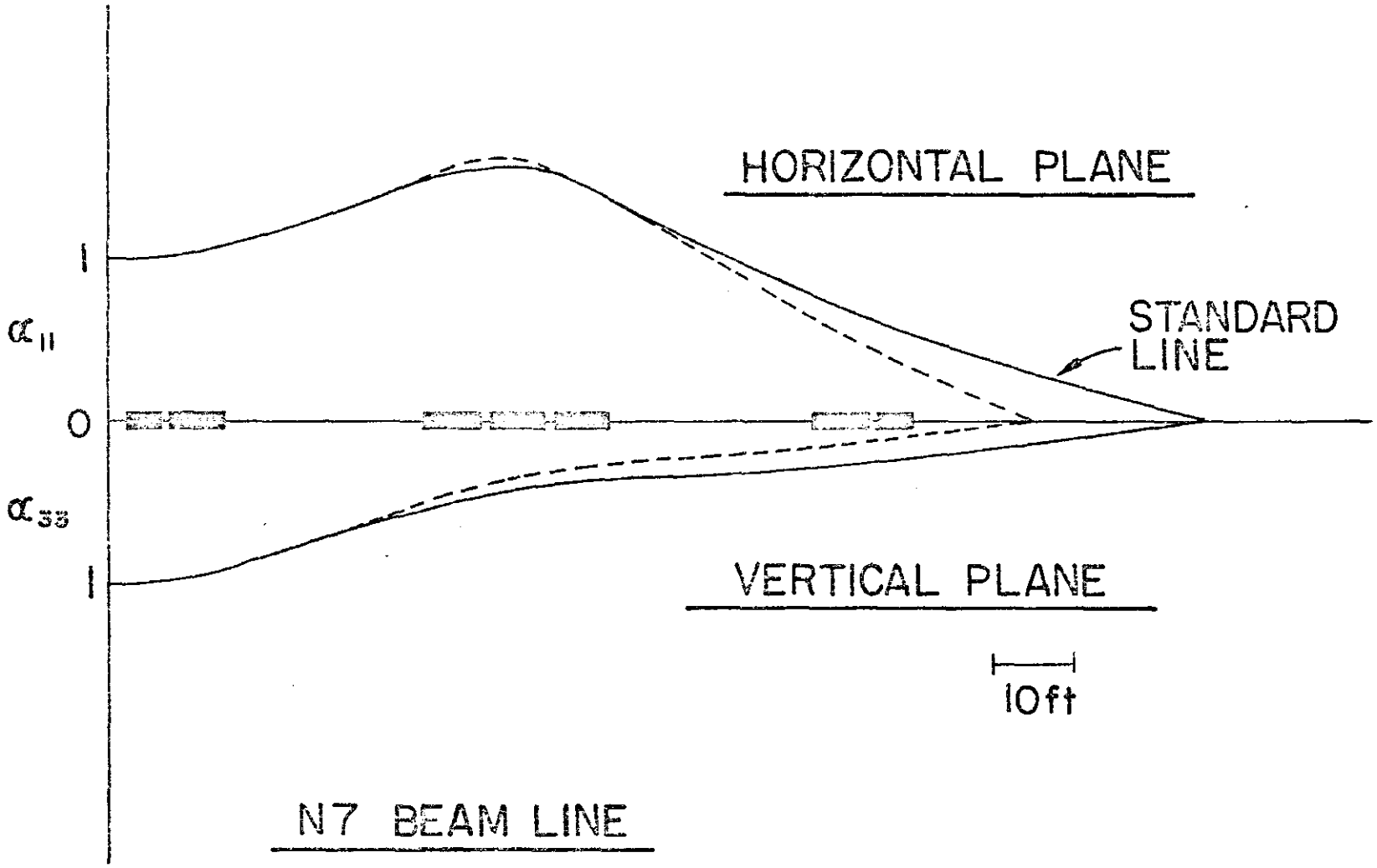
HORIZONTAL PLANE
STANDARD LINE
1
α_{11}
0
α_{33}
1
VERTICAL PLANE
10ft
N7 BEAM LINE

FIGURE 10

FIGURE II

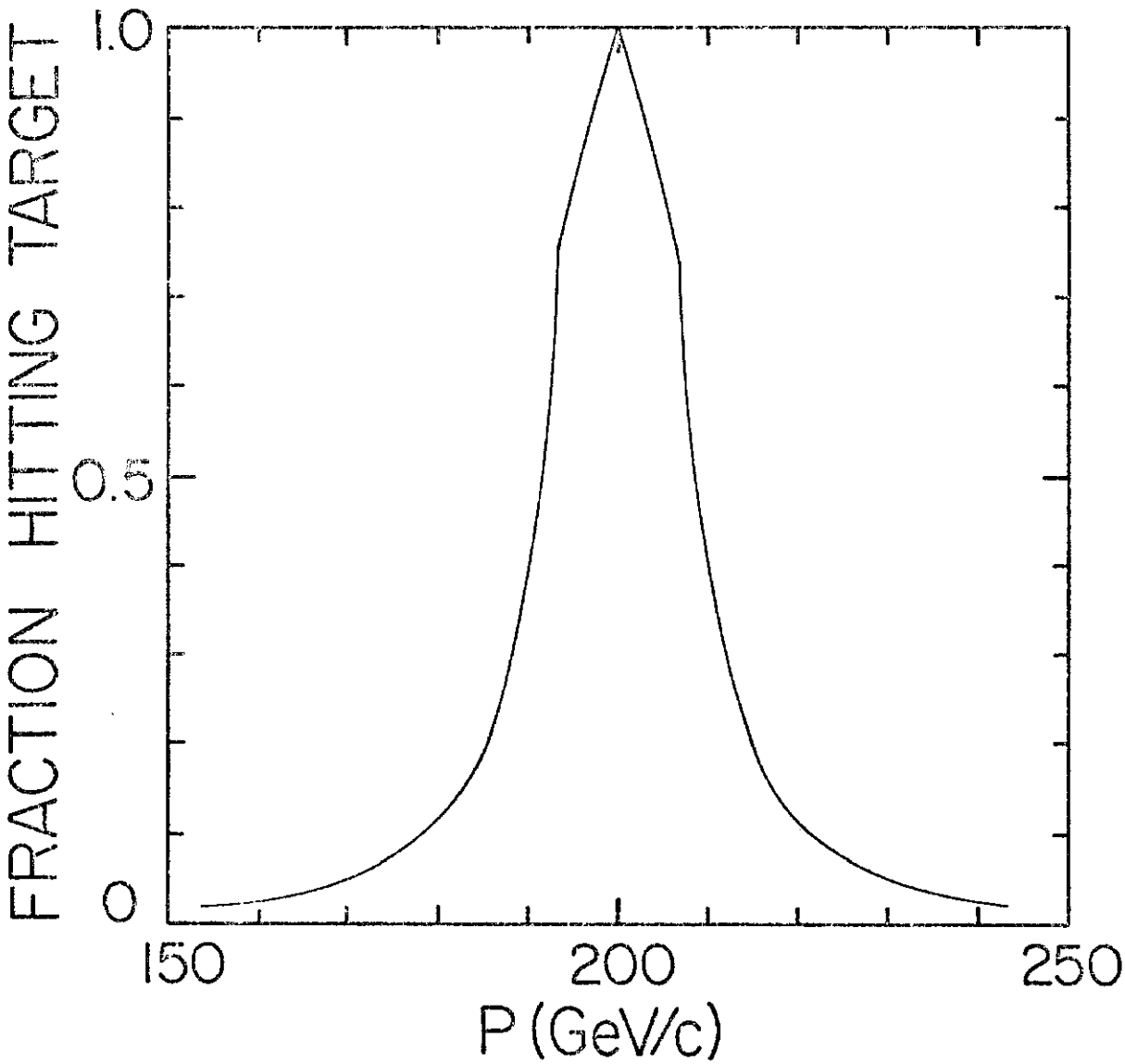

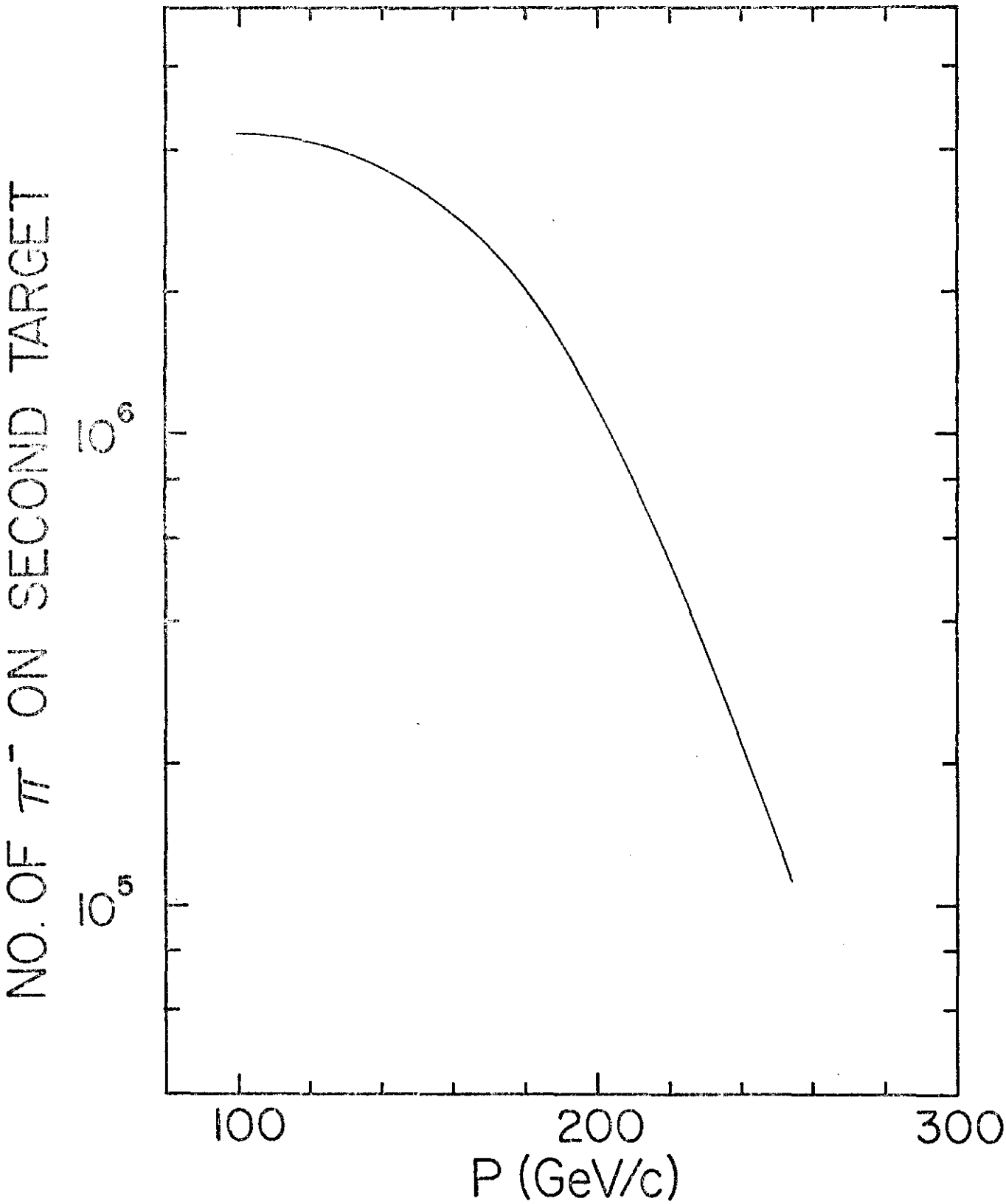

FIGURE 12

FIGURE 13

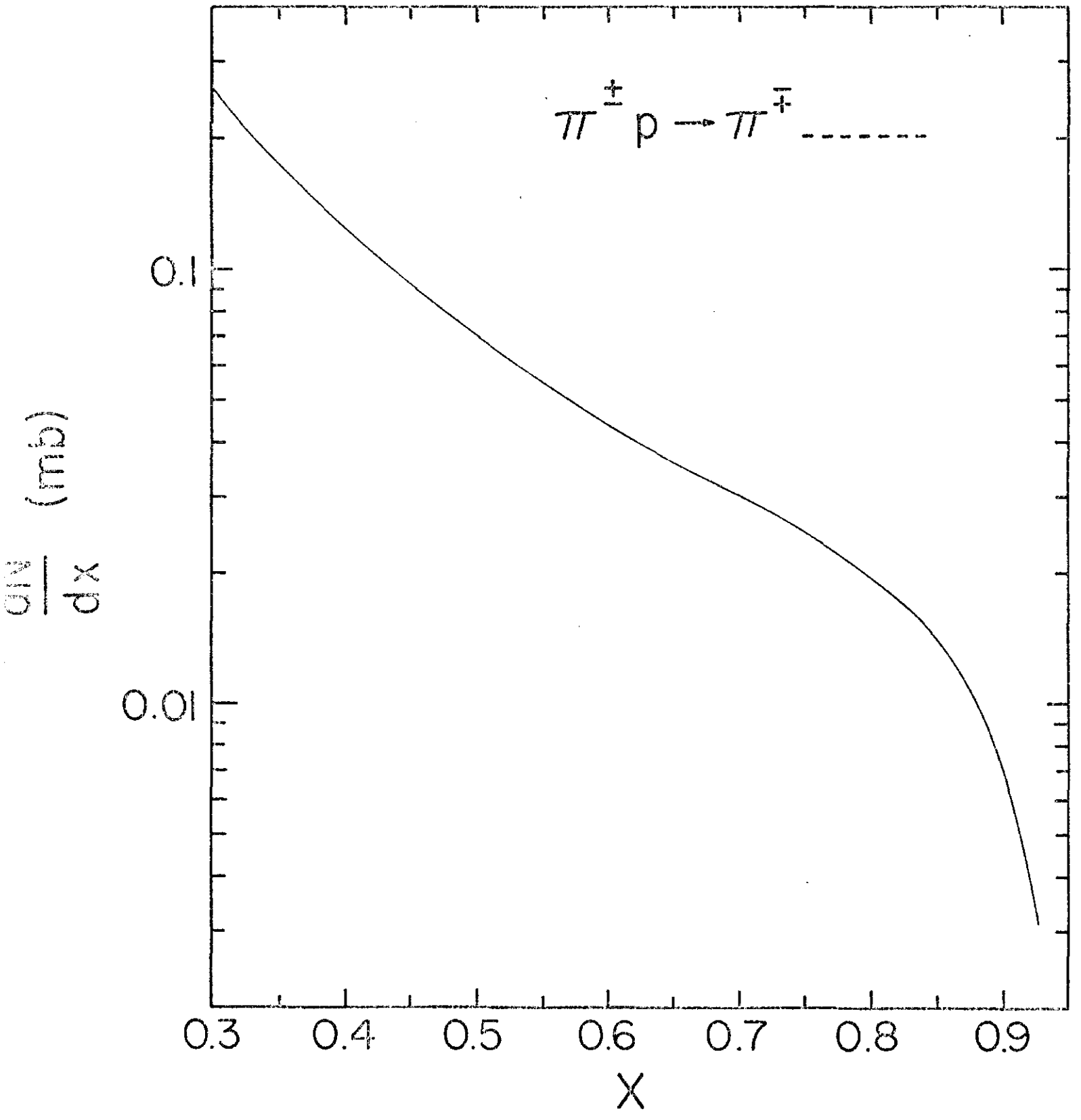
$\pi^{\pm} p \rightarrow \pi^{\mp}$ ------
0.1
0.01
$\frac{d\sigma}{dx}$ (mb)
0.3
0.4
0.5
0.6
0.7
0.8
0.9
X

FIGURE 14

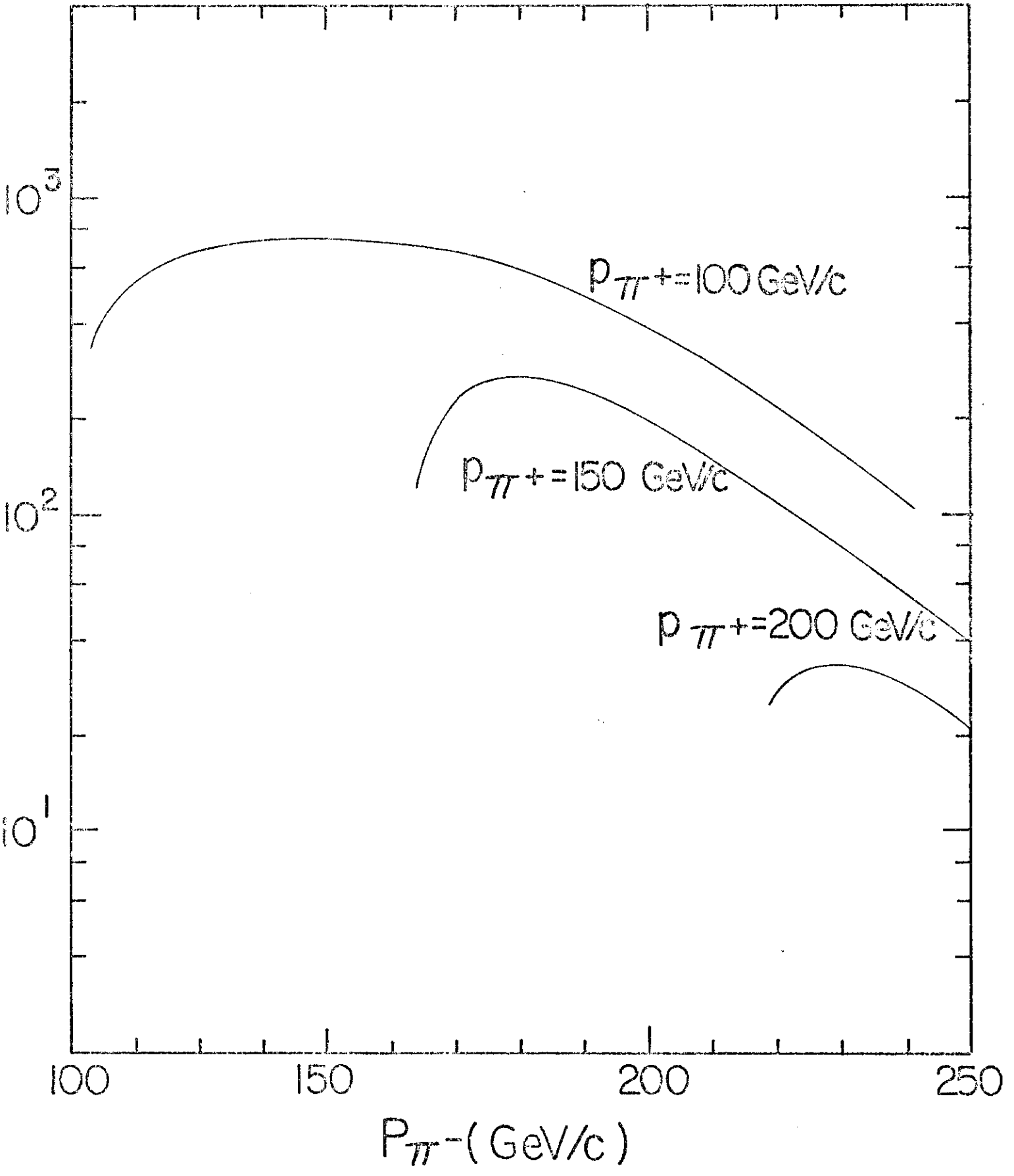
10^3
10^2
10^1
p_{π^+}=100 GeV/c
p_{π^+}=150 GeV/c
p_{π^+}=200 GeV/c
100
150
200
250
P_{π^-} (GeV/c)

FIGURE 15

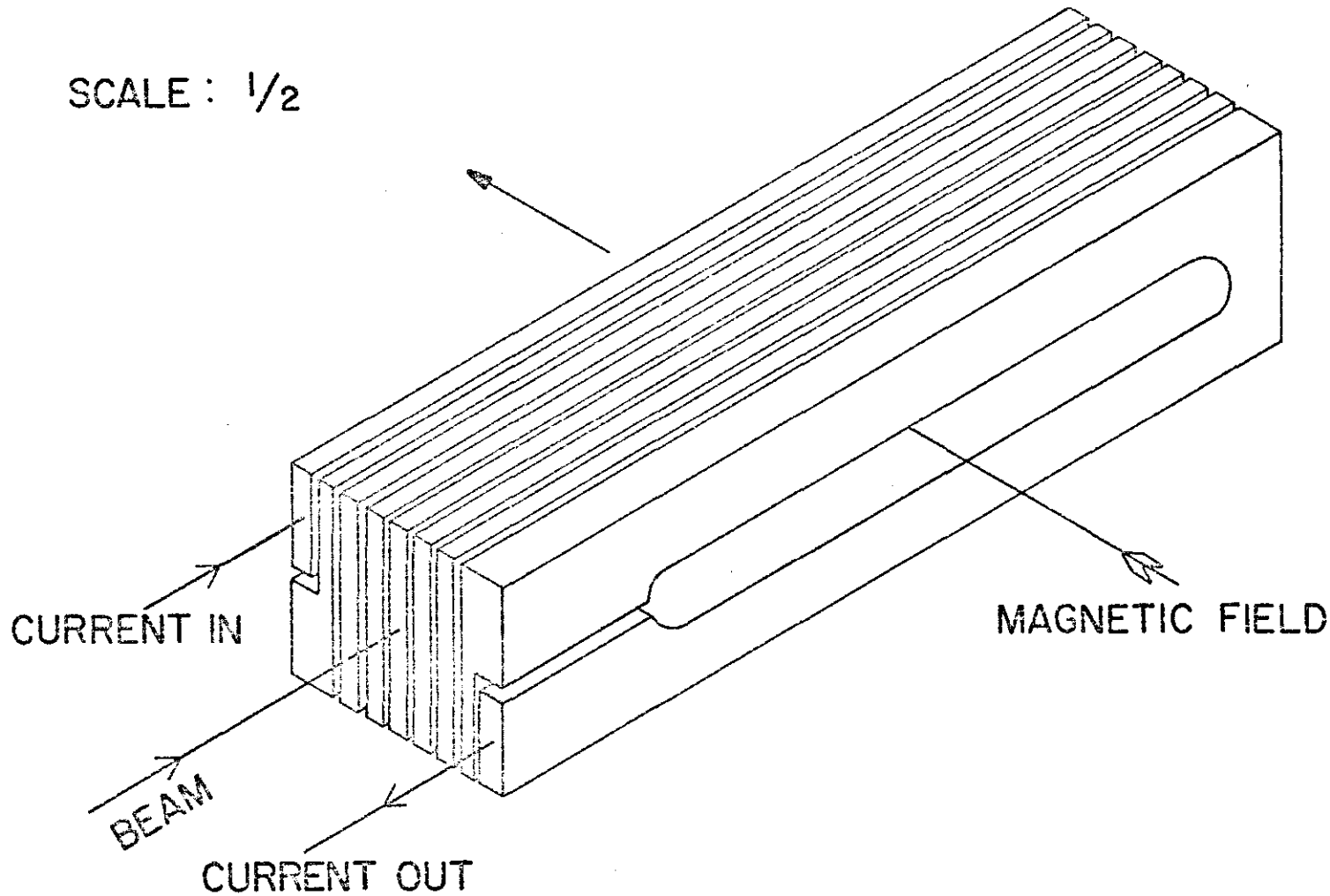

PULSED DIPOLE COIL

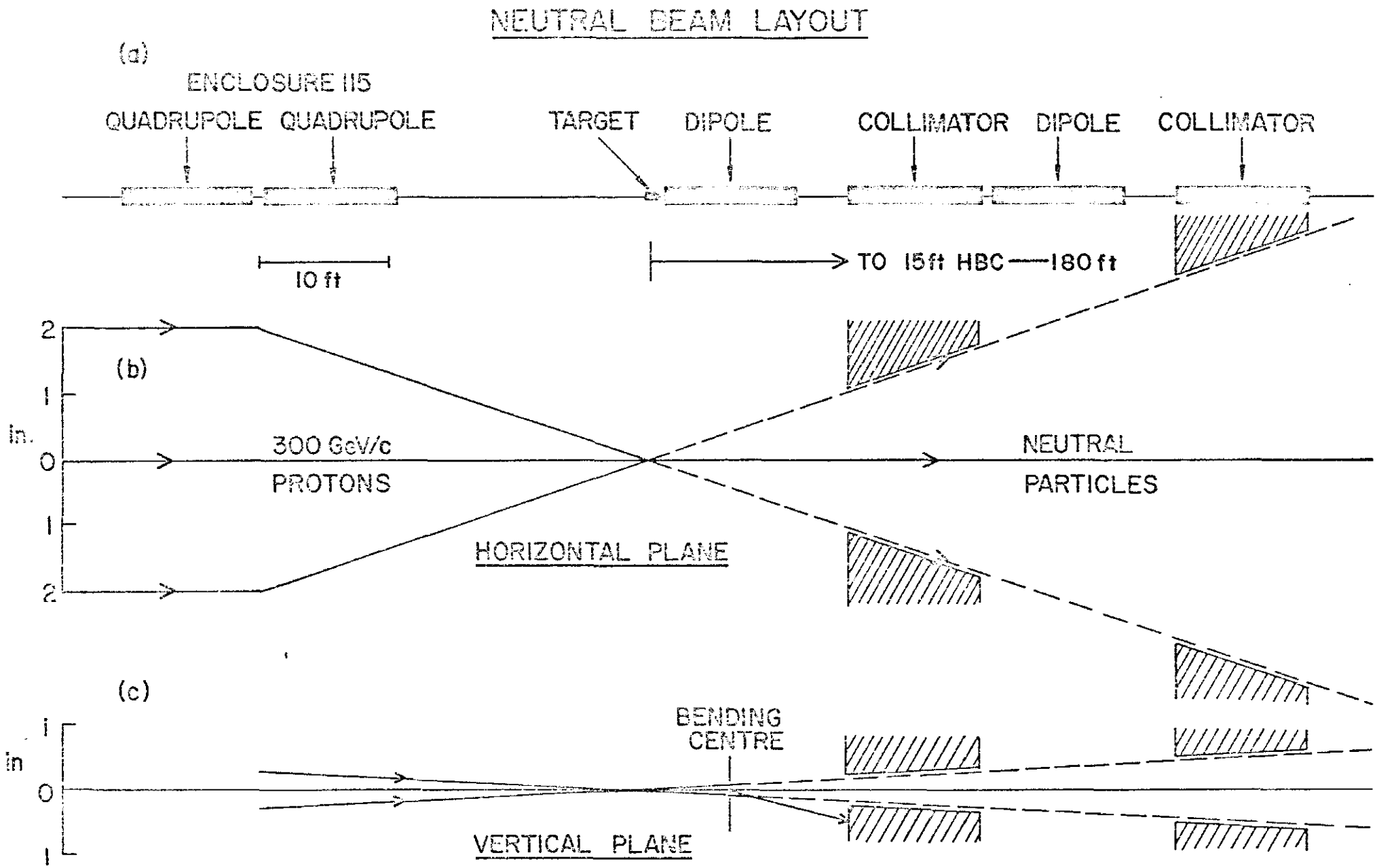
NEUTRAL BEAM LAYOUT
(a)
ENCLOSURE 115
QUADRUPOLE
QUADRUPOLE
TARGET
DIPOLE
COLLIMATOR
DIPOLE
COLLIMATOR
10 ft
TO 15ft HBC
180 ft
(b)
2
1
0
1
2
in.
300 GeV/c
PROTONS
NEUTRAL
PARTICLES
HORIZONTAL PLANE
(c)
1
0
1
in
BENDING
CENTRE
VERTICAL PLANE

FIGURE 16

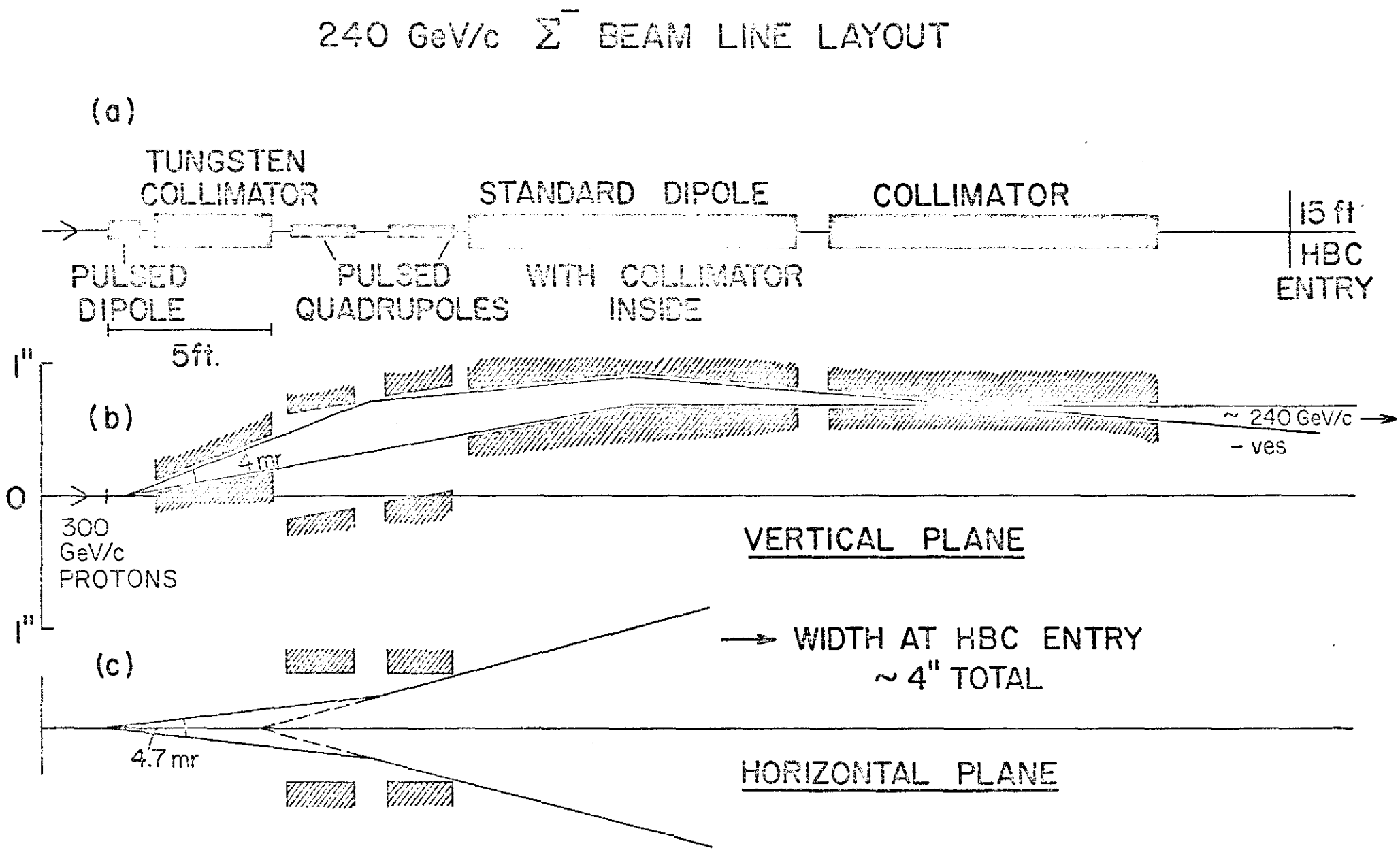
240 GeV/c Σ⁻ BEAM LINE LAYOUT
(a)
TUNGSTEN COLLIMATOR
STANDARD DIPOLE
COLLIMATOR
15 ft
HBC ENTRY
PULSED DIPOLE
PULSED QUADRUPOLES
WITH COLLIMATOR INSIDE
5ft.
1"
(b)
4 mr
~ 240 GeV/c
- ves
0
300 GeV/c PROTONS
VERTICAL PLANE
1"
(c)
WIDTH AT HBC ENTRY
~ 4" TOTAL
4.7 mr
HORIZONTAL PLANE

FIGURE 17

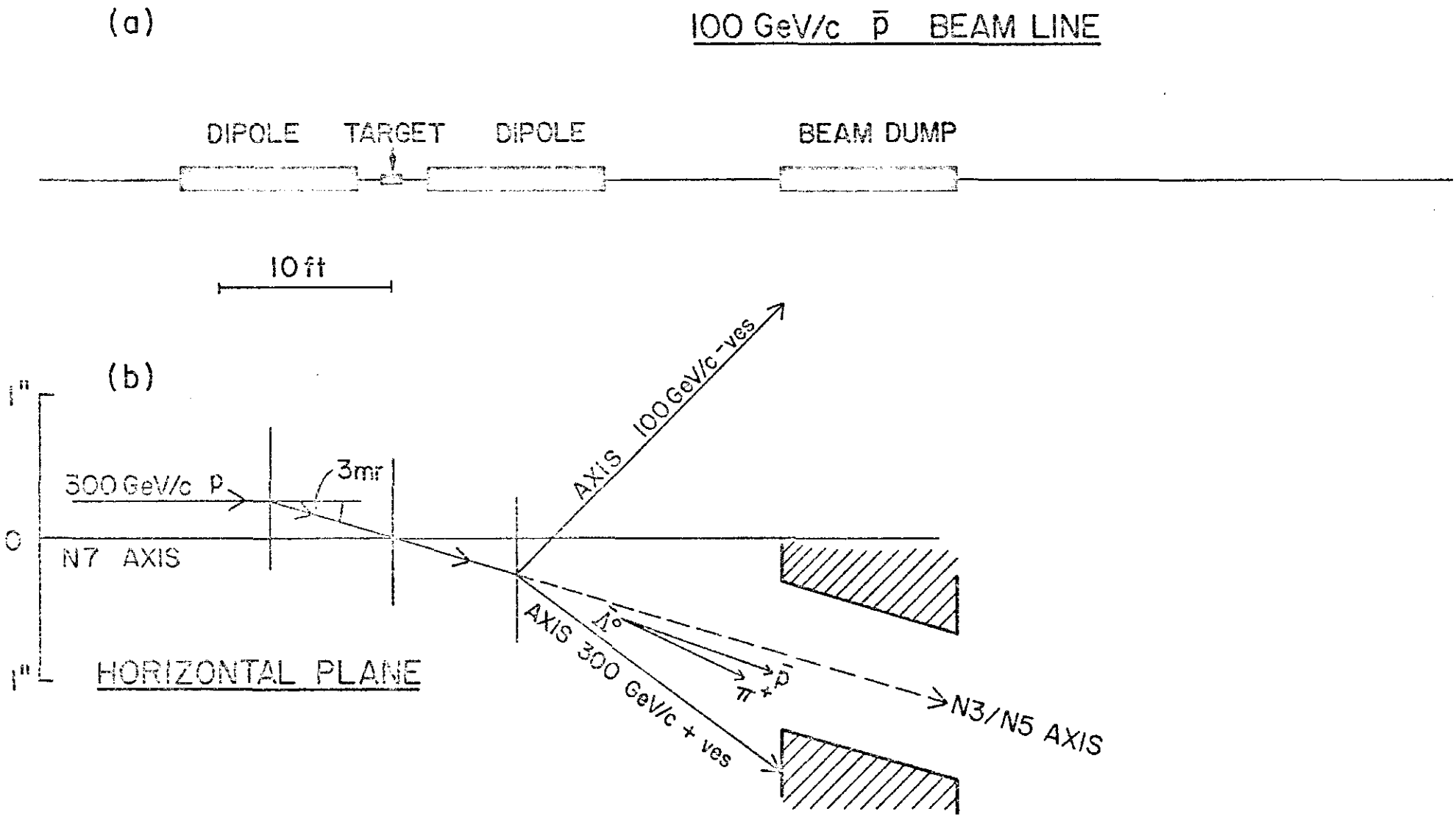
(a)
100 GeV/c $\bar{p}$ BEAM LINE
DIPOLE
TARGET
DIPOLE
BEAM DUMP
10 ft
(b)
1"
0
1"
300 GeV/c P
3mr
N7 AXIS
AXIS 100 GeV/c -ves
AXIS 300 GeV/c + ves
$\bar{\Lambda}^0$
π^+
$\bar{p}$
N3/N5 AXIS
HORIZONTAL PLANE

FIGURE 18

FIGURE 19

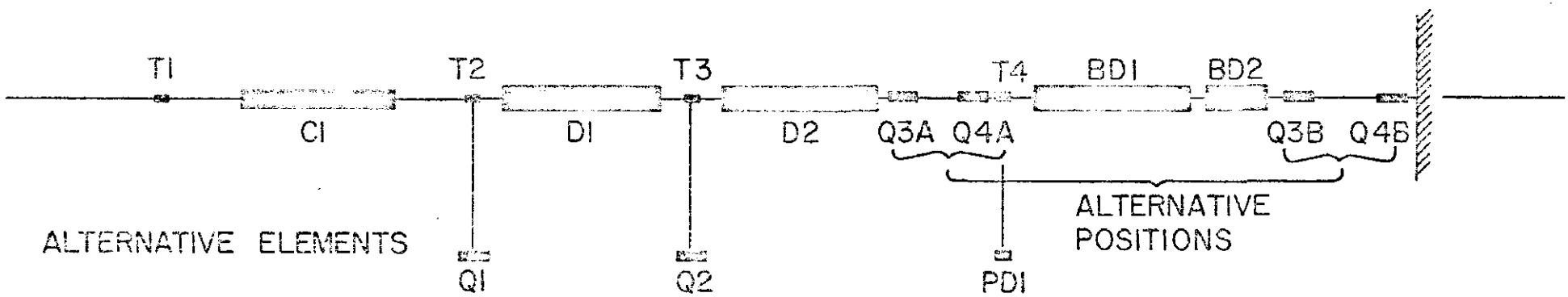

KEY: T — TARGET
C — COLLIMATOR
BD — BEAM DUMP
D — STANDARD DIPOLE
Q — PULSED QUADRUPOLE

FACILITY LAYOUT
IN ENCLOSURE 100

10 ft